International Journal of Mechanics and Energy (IJME)
Vol. 2, Issue 3, 2014, ISSN: 2286-5845

Finite Element Analysis of ECAE Deformation of Polycarbonate

F. Bouaksa[1,2], C.M. Ovalle-Rodas[1], F. Zaïri[1], M. Naït-Abdelaziz[1], T. Tamine[2],

[1]Université Lille 1 Sciences et Technologies, Laboratoire de Mécanique de Lille (LML), UMR CNRS 8107, F-59650 Villeneuve d'Ascq, France

[2]Université des Sciences et de la Technologie d'Oran, Laboratoire de Carburant Gazeux et Environnement (LCGE), BP-1505 El-M'naouar, Algérie

Abstract: The behavior of molecularly orientated polycarbonate (PC) sheets was investigated numerically. In the present contribution finite element simulations, using a physically-based viscohyperelastic-viscoplastic constitutive model, were carried out in order to evaluate the degree and distribution of molecular chain anisotropy in polycarbonate and the effect of strain rate on distribution of plastic deformation when it is extruded by the ECAE process at 135°.

Key words: FEM, ECAE , molecular orientation

1. Introduction

Variuos techniques have been developed to obtain such mechanical properties. One such technical, the Equal Channel Angular Extrusion (ECAE) . In ECAE, the workpiece is pressed through a die that contains two channels with equal cross-section meeting at angle Φ, having corner angle Ψ as shown in Fig 1. Since the cross-section of the workpiece remains unchanged. ECAE is an innovative process which has attracted a lot of attention in recent years and many papers have been published dealing with this subject.

This ECAE process was originated by Segal and colleagues in the 1980s [1] their objective when designing the process at that time, was to develop a metal forming process with a high strain rate. One important advantage of the ECAE process is that it can be repeated several times without changing the dimensions of the workpiece, and the applied strain can be increased to any level; these advantages mean that the severe strains that can be applied and a simple shear deformation mode contribute to the strong and unusual properties of the material produced.

ECAE technique was applied to a wide range of thermoplastic polymers such as polycarbonate, polymethylmethacrylate, the high density polyethylene, polypropylene, Polyethylene-terephthalate semi crystalline nylon-6, nylon-12 and polyacetal [2-16].

Some works were found on the extrusion of polycarbonate, for example, the analysis of [7] highlights the effectiveness of ECAE process on changing the mechanical properties of polycarbonate (PC), namely the flexural modulus and fracture toughness. Also, the enhancement of the fracture resistance of extruded polycarbonate samples was pointed out by [8] and et al [9].More recently, the effect of ECAE on the mechanical response of the same material was investigated by [12].

* **Corresponding author:** Fethia BOUAKSA
E-mail: fbouaksa@yahoo.fr

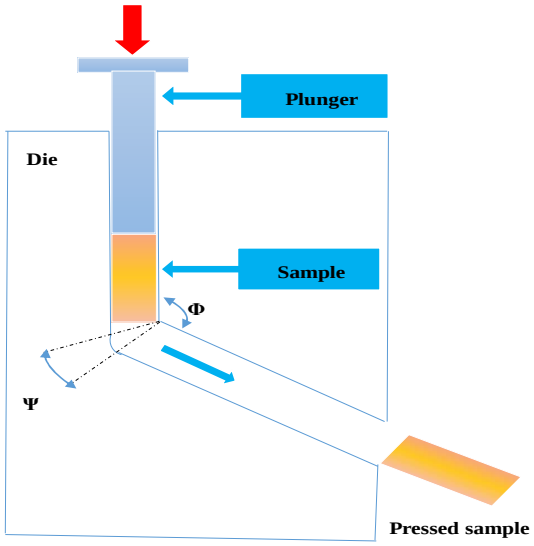

Fig. 1. Schematic illustration of the ECAE process

In the present contribution finite element simulations, using a physically-based constitutive model, were carried out in order to evaluate the degree and distribution of molecular chain anisotropy in polycarbonate when it is extruded by the ECAE with channel angle of 135°.

2. Numerical study

2.1 Material model and identification

The (PC) material used in this study is a polycarbonate purchased from the Goodfellow Company. The stress – strain behavior of PC was characterized under uniaxial tension on an electromechanical testing machine (Instron © mode 5800). The local strain was measured using a video-controlled system (VideoTraction ©) consisting of a CCD camera interfaced with a computer. This system of strain measurement was developed (G'Sell et al. 2002). The tensile specimens were cut from plates of 2 mm thick (Fig.2.a). A curvature radius of 60 mm was imposed in the central part of the test piece to locate the deformation in section while retaining the stress triaxiality in the order of 0.33. Seven markers are printed prior to deformation on the front surfaces of the sample. In the present case the markers are black, nearly round, with a diameter of about 0.4 mm. The diagram in (Fig.2. b.) illustrates their configuration after necking has developed. The tensile tests were performed at different speeds of solicitation (10-2, 10-3 et 10-4 (s-1)), and at ambient temperature.

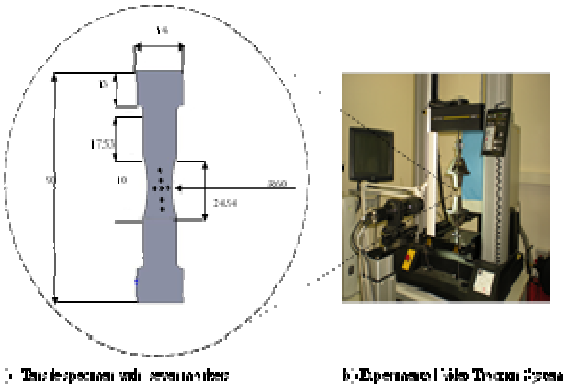

Fig. 2. A system for measuring deformation and geometric characteristics of the specimens during a video-controlled tensile test

2.2 FE Model

In the first part of this section, a viscohyperelastic-viscoplastic modeling was adopted and implemented into a computer code (Marc-MSC) for capturing the stress-strain behavior of polycarbonate (PC). In the second part we present the simulation of the model in ECAE.

2.2.1. kinematics

In the framework of the theory for the large inelastic deformation kinematics, we consider the deformation gradient tensor $\mathbf{F} = \nabla \mathbf{x}(\mathbf{X}, t)$ where $\mathbf{X}$ is the position of material point in the reference configuration to its actual position $\mathbf{x}$ in the current configuration. Following the approach proposed by Lee [17] elastic-(visco) plastic decomposition or the Sidoroff [18] visco-(hyper)elastic decomposition, the total imposed deformation gradient $\mathbf{F}$ can be decomposed in a multiplicative manner into an elastic

$\mathbf{F}^{el}$ part and an inelastic (viscoplastic or viscous) $\mathbf{F}^{inel}$ part:

$$\mathbf{F} = \mathbf{F}^{el}\mathbf{F}^{inel} \tag{2}$$

The time derivative of the total, elastic and inelastic deformation gradients can be also introduced:

$$\dot{\mathbf{F}} = \mathbf{L}\mathbf{F}\,,\quad \dot{\mathbf{F}}^{el} = \mathbf{L}^{el}\mathbf{F}^{el} \text{ and } \dot{\mathbf{F}}^{inel} = \mathbf{L}^{inel}\mathbf{F}^{inel} \tag{3}$$

in which the dot denotes the time derivative.

The gradient $\mathbf{L} = \nabla\mathbf{v}$ of the spatial velocity $\mathbf{v} = \dot{\mathbf{x}}\mathbf{x}^{-1}$ can be decomposed in an additive manner into an elastic $\mathbf{L}^{el}$ part and an inelastic $\mathbf{L}^{inel}$ part:

$$\mathbf{L} = \mathbf{L}^{el} + \mathbf{L}^{inel} = \mathbf{L}^{el} + \mathbf{F}^{el}\mathbf{L}^{inel}\mathbf{F}^{el^{-1}} \tag{4}$$

The elastic and inelastic velocity gradients $\mathbf{L}^{el}$ and $\mathbf{L}^{inel}$ are given by:

$$\mathbf{L}^{el} = \dot{\mathbf{F}}^{el}\mathbf{F}^{el^{-1}} = \mathbf{D}^{el} + \mathbf{W}^{el} \quad \text{and}$$

$$\mathbf{L}^{inel} = \mathbf{F}^{el}\dot{\mathbf{F}}^{inel}\mathbf{F}^{inel^{-1}}\mathbf{F}^{el^{-1}} = \mathbf{D}^{inel} + \mathbf{W}^{inel} \tag{5}$$

where $\mathbf{D} = \mathbf{D}^{el} + \mathbf{D}^{inel}$ and $\mathbf{W} = \mathbf{W}^{el} + \mathbf{W}^{inel}$ represent the stretching rate and the spin rate, respectively. The inelastic flow is assumed volume preserving, i.e. $\det\mathbf{F}^{inel} = 1$. Assuming, without loss of generality, the inelastic flow irrotational, i.e. $\mathbf{W}^{inel} = \mathbf{0}$, the relation (5) gives the evolution equation of the inelastic deformation gradient $\mathbf{F}^{inel}$:

$$\dot{\mathbf{F}}^{inel} = \mathbf{F}^{el^{-1}}\mathbf{D}^{inel}\mathbf{F}^{el}\mathbf{F}^{inel} = \mathbf{F}^{el^{-1}}\mathbf{D}^{inel}\mathbf{F} \tag{6}$$

Once the inelastic deformation gradient $\mathbf{F}^{inel}$ computed by integrating the relation (6), the elastic deformation gradient $\mathbf{F}^{el}$ is then extracted from the relation (2).

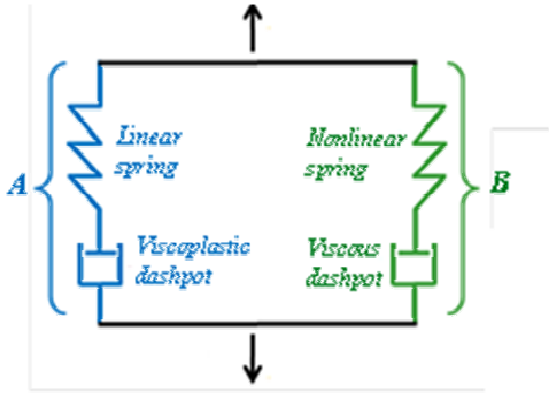

Fig. 3. Schematic visualization of the constitutive model

2.2.2. Constitutive relations

In what follows, the three-dimensional constitutive equations, expressing the inelastic stretching rate as a function of the stress in the material, are described for the two branches. The subscript A and B will be used to differentiate the two branches. The constitutive model being constructed with the Taylor assumption (i.e. parallelism of the two branches), the deformation gradients within the two branches, $\mathbf{F}_A$ and $\mathbf{F}_B$, are identical to the total deformation gradient $\mathbf{F}$, i.e. $\mathbf{F}_A = \mathbf{F}_B = \mathbf{F}$. Moreover, the total Cauchy stress $\mathbf{T}$ is the sum of the Cauchy stresses $\mathbf{T}_A$ and $\mathbf{T}_B$ in each branch : $\mathbf{T} = \mathbf{T}_A + \mathbf{T}_B$.

The inelastic stretching rates $\mathbf{D}_A^{inel}$ and $\mathbf{D}_B^{inel}$ for the branches A and B, respectively, are given by the following general flow rules:

$$\mathbf{D}_A^{inel} = \dot{\gamma}_A^{inel}\mathbf{N}_A^{inel} \quad \text{and} \quad \mathbf{D}_B^{inel} = \dot{\gamma}_B^{inel}\mathbf{N}_B^{inel} \tag{7}$$

in which $\dot{\gamma}^{inel}$ is the inelastic shear strain rate described below and $\mathbf{N}^{inel}$ is the direction tensor of $\mathbf{D}^{inel}$ aligned with the deviatoric Cauchy stress $\mathbf{T}'$:

$$\mathbf{N}_A^{inel}=\frac{\mathbf{T}'_A}{\sqrt{2}\tau_A} \quad \text{and} \quad \mathbf{N}_B^{inel}=\frac{\mathbf{T}'_B}{\sqrt{2}\tau_B} \tag{8}$$

where τ is the effective shear stress related to the deviatoric Cauchy stress $\mathbf{T}'=\mathbf{T}-\text{trace}(\mathbf{T})/3\mathbf{I}$:

$$\tau_A=\sqrt{\frac{1}{2}\mathbf{T}'_A.\mathbf{T}'_A} \quad \text{and} \quad \tau_B=\sqrt{\frac{1}{2}\mathbf{T}'_B.\mathbf{T}'_B} \tag{9}$$

in which the dot denotes the tensor product: $\mathbf{A}.\mathbf{B}=\text{tr}(\mathbf{A}^T\mathbf{B})$, $\mathbf{A}^T$ being the transpose of $\mathbf{A}$.

2.2.3 Branch A: Polymer intermolecular response

The Cauchy stress of the branch A is given by the following relation:

$$\mathbf{T}_A=\frac{1}{J_A^{el}}\mathbf{C}_A^{el}\ln(\mathbf{V}_A^{el}) \quad \text{with} \quad \mathbf{V}_A^{el}=\mathbf{F}_A^{el}\mathbf{R}_A^{el^{-1}} \tag{10}$$

where $J_A^{el}=\det\mathbf{F}_A^{el}$ is the elastic volume change, $\ln(\mathbf{V}_A^{el})$ is the Hencky strain, $\mathbf{V}_A^{el}$ is the elastic stretch, $\mathbf{R}_A^{el}$ is the elastic rotation and $\mathbf{C}_A^{el}$ is the fourth-order tensor of elastic constants expressed, for an isotropic material, in function of the Young's modulus E_A and the Poisson's ratio ν_A:

$$\left(C_A^{el}\right)_{ijkl}=\frac{E_A}{2(1+\nu_A)}\left[\left(\delta_{ik}\delta_{jl}+\delta_{il}\delta_{jk}\right)+\frac{2\nu_A}{1-2\nu_A}\delta_{ij}\delta_{kl}\right] \tag{11}$$

where the term δ denotes the Kronecker-delta symbol.

The inelastic (viscoplastic) shear strain rate $\dot{\gamma}_A^{inel}$ follows an Arrhenius type expression [31]:

$$\dot{\gamma}_A^{inel}=\gamma_0\exp\left[-\frac{\Delta G}{k\theta}\left(1-\frac{\tau_A}{s}\right)\right] \tag{12}$$

where k is the Boltzmann's constant, θ is the absolute temperature, γ_0 is a pre-exponential shear rate factor, ΔG is the activation energy which must be overcome for flow to begin and s is the athermal shear strength taken to evolve with inelastic straining to account for the strain softening according to the following equation:

$$\dot{s}=h\left(1-\frac{s}{s_s}\right)\dot{\gamma}_A^{inel}, \quad s(t=0)=s_0 \tag{13}$$

in which h is the slope of the yield drop with respect to inelastic strain, s_0 is the initial value of s and s_s is the saturation value of s.

2.2.4. Branch B: Stretching and chain orientation

The molecular network of the polymeric material is initially isotropic, but tends to align along the direction of principal stretch during the large inelastic deformation. This is the commonly accepted rubbery network-like response of glassy polymers to inelastic deformation, which results in the dramatic strain hardening in the mechanical response. The strain hardening response can be captured by a purely descriptive phenomenological approach or a statistical (physically-based) approach. The physically-based approach integrates in its formulation the molecular network properties and uses the extensibility limit of polymer chains as a measure of deformation. The Cauchy stress $\mathbf{T}_B$ of the branch B is expressed by a physically-based

relation using the inverse Langevin function to account for the limiting chain extensibility [31]:

$$\mathbf{T}_B = \frac{1}{J_B^{el}} \frac{C_r}{3} \frac{\sqrt{N}}{\bar{\lambda}_B^{el}} \mathcal{L}^{-1}\left(\frac{\bar{\lambda}_B^{el}}{\sqrt{N}}\right)\left[\bar{\mathbf{B}}_B^{el} - \left(\bar{\lambda}_B^{el}\right)^2 \mathbf{I}\right] \quad (14)$$

where $\mathcal{L}^{-1}$ is the inverse Langevin function which can be estimated using the Padé approximation [37]: $\mathcal{L}^{-1}(x) = x\left(3-x^2\right)/\left(1-x^2\right)$.

The term $J_B^{el} = \det \mathbf{F}_B^{el}$ is the elastic volume change. The relation (14) introduces two network parameters: the average number of chains per unit volume n (introduced in the rubbery modulus $C_r = nk\theta$) and the number of rigid links between physical molecular chain entanglements N. The term $\sqrt{N}$ represents the limiting extensibility of the polymer chains; if the chain stretch approaches this limit the stress increases dramatically. Note that if this term approaches infinity the relation (14) reduces to the classical Neo-Hookean model, involving no dramatic strain hardening. The term $\bar{\lambda}_B^{el} = \sqrt{\text{trace}\left(\bar{\mathbf{B}}_B^{el}\right)/3}$ is the stretch on each chain in the network, $\bar{\mathbf{B}}_B^{el} = \bar{\mathbf{F}}_B^{el}\left(\bar{\mathbf{F}}_B^{el}\right)^T$, where $\bar{\mathbf{F}}_B^{el} = \left(J_B^{el}\right)^{-1/3}\mathbf{F}_B^{el}$, is the elastic left Cauchy-Green tensor.

In addition to the stretching and chain orientation process, a molecular relaxation process is included in the model formulation from the inelastic (viscous) shear strain rate $\dot{\gamma}_B^{inel}$ [19]:

$$\dot{\gamma}_B^{inel} = C\left(\frac{1}{\lambda_B^{inel} - 1}\right)\tau_B \quad (15)$$

where $\lambda_B^{inel} = \sqrt{\text{trace}\left(\mathbf{B}_B^{inel}\right)/3}$, $\mathbf{B}_B^{inel} = \mathbf{F}_B^{inel}\left(\mathbf{F}_B^{inel}\right)^T$ being the inelastic left Cauchy-Green tensor and C is a viscosity parameter introduced because of the physics of chain relaxation.

In order to ensure numerical stability due to singularity of Eq. (15) at the beginning of the loading process where λ_B^{inel} = 1, a perturbation coefficient κ is added to λ_B^{inel} (κ = 0.01 is taken throughout our simulations).

2.2.5 Identification of the model parameters

The model parameters, used as input data in the subroutine, were identified from the set of stress-strain curves shown in Fig. 4. A fairly good agreement was observed between the identified constitutive model and experimental results. After identification of parameters, E_A and ν_A, in the elastic region, the parameters γ_0, ΔG and s_0 were identified from a least-squares adjustment of the yield stress over the strain rates. The other parameters (s_s, h, N and C_r) involved in the model were estimated by simulating a tensile tests on a cube deformed until 100% for the whole range of strain rates used range of 10-2, 10 -3 and 10-4 (s-1). The parameters s_s and h characterize the strain softening region, whereas the parameters C_r, N and C were fitted in the strain hardening region. The identified values are listed in Table 1.

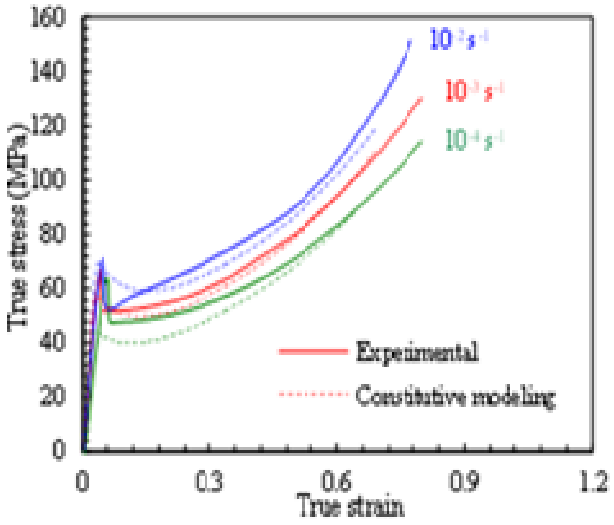

Fig. 4. Comparison between experimental and FEM results for stress-strain curves.

Table1. Material parameter of PC.

Parameter		Value
E_A	MPa	2200
ν_A		0.4
s_0	MPa	74.5
s_s	MPa	40
h	MPa	500
γ_0	s^{-1}	10^4
ΔG	J	1.07×10^{-19}
N		8.0
C_r	MPa	29.0
C	$MPa^{-1}.s^{-1}$	1.11×10^{-10}

3. Simulation of ECAE

The deformation behavior of a square cross-sectioned polycarbonate sample with dimension 10X10X75 mm3 (width x thickness x length) in an ECAE die with a channel at 135° was simulated using (Marc-MSC) under plane strain conditions at room temperature. The deformable work piece was meshed with 4-node quadrilateral elements. The friction between the specimen and the die channels was modeled using the Coulomb's friction law and a friction coefficient of 0.1 was chosen. The die and the ram were assumed to be rigid. As the ECAE process combines large displacement and large strain, an updated Lagrangian procedure has been used.

4. Results and discussion.

Fig 5. Shows the actual values of the force required for pressing 10x10x75 mm^3 parallelepipedic bars of PC at different values of strain rates (10-2, 10-3,10-4) s-1, The force required for each speed in the ascending order (7.139, 4.168,3.99) kN. Another interesting point is the load versus ram displacement evolution during the process, which can be subdivided into three main stages. The first stage starts from the origin up to the maximum. This stage corresponds to development zone of inelastic deformation and the absence of the viscoplastic strain. The second stage corresponds to the softening phase whose stress decreases until saturation stress, characteristic of the plastic flow stress. In the last stage, viscoplastic contribution increases and the material hardens gradually following the orientation of the macromolecules along the extrusion direction.

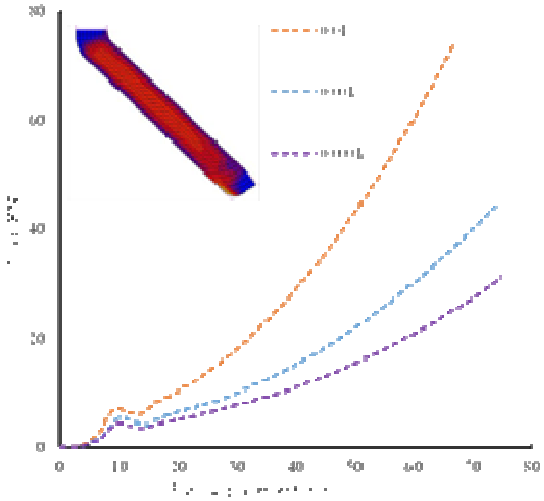

Fig. 5. Variation of the load versus displacement for the three speeds (10^{-2} 10^{-3} 10^{-4} (s^{-1})).

Fig 6, show the color bands distribution from the full 2-D analysis to the intermolecular and molecular network stresses. they show a regional gradient from the inner to the outer arc. However, it is also clear that the stress state is multiaxial and inhomogeneous.

Along the specimen length, there is a steady plastic flow region where the intermolecular stress components seem uniform.

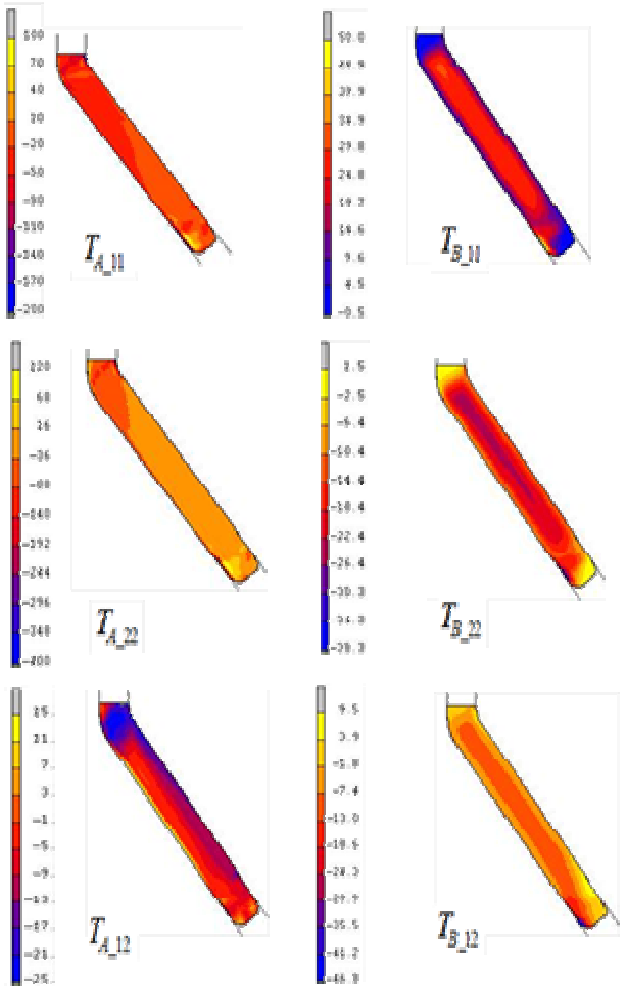

Fig. 6. Stress fields of the two branches (*A* and *B*) at the end of the ECAE at $10^{-2}(s^{-1})$.

The distribution of the equivalent plastic strain distribution along the workpiece length after ECAE process is shown in Fig 7 (a-b). it can be seen that the faster the ram speed is , the higher the homogeneity of the equivalent plastic strain distribution is, as it is clear in the fig.8

Where the distribution has been traced to a point at the center of the sample in according to the ram displacement for three ram speeds . It was also noticed that the influence of this parameter is slight and a better result can be obtained when the ram speed is 0.001 (s^{-1}).

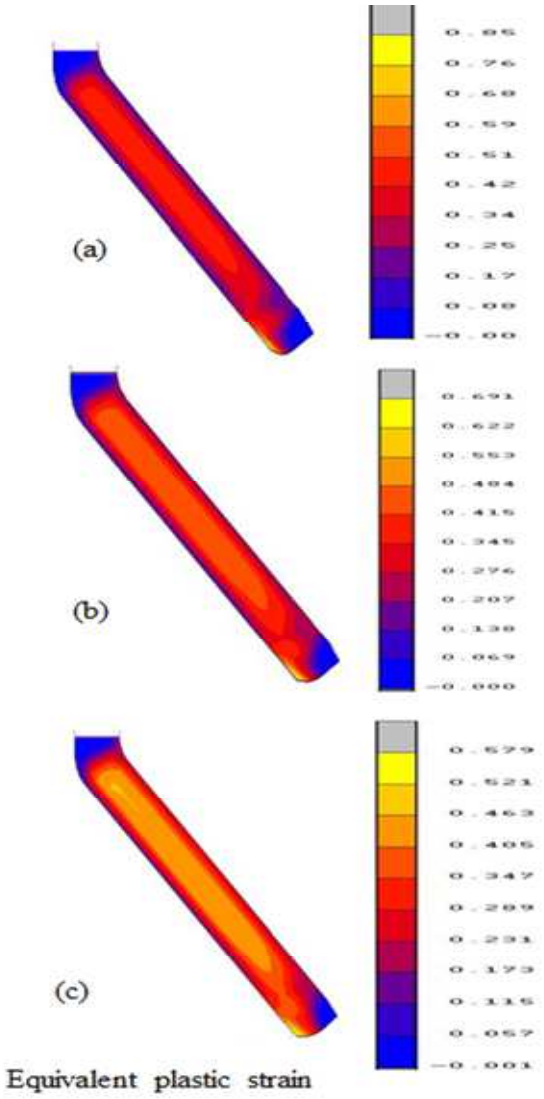

Fig. 7. Equivalent plastic strain along the workpiece length after ECAE 135° at three speeds respectively (10^{-2} 10^{-3} 10^{-4} (s^{-1})).

Distribution of plastic deformation was plotted then in the center of the room and in throughout the thickness as shown in Fig 9., from the latter it has been noticed , the accordance with the value found from literature by the analytical formula [4] and that obtained by simulation.

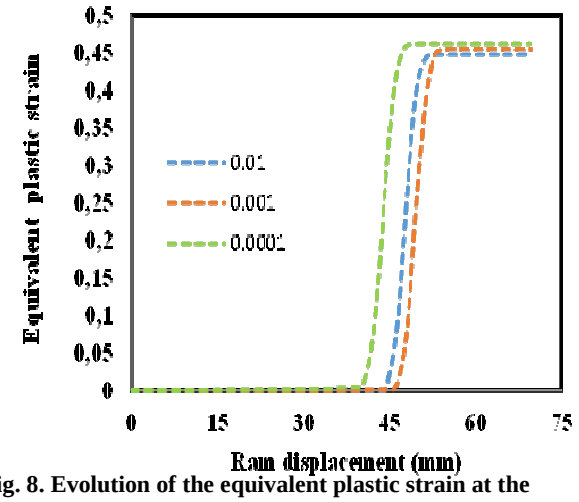

Fig. 8. Evolution of the equivalent plastic strain at the center of the sample (10^{-2} 10^{-3} 10^{-4} (s^{-1})).

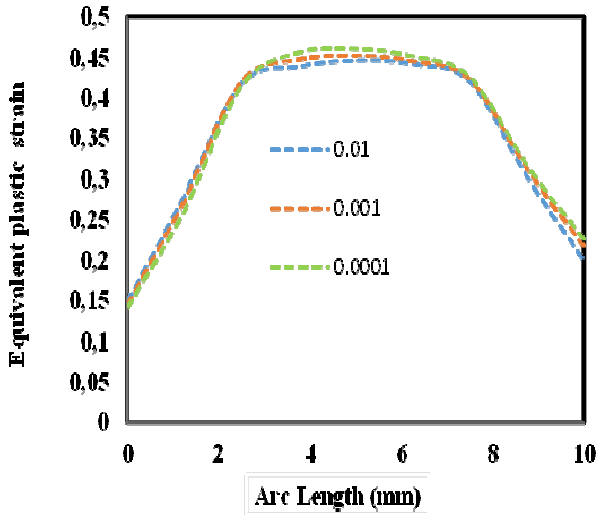

Fig. 9. Equivalent plastic strain distribution along the sample thickness at respectively (10-2 10-3 10-4 (s-1)).

4. Conclusion

In order to investigate the evolution of molecular chain orientation in polycarbonate when it is extruded by the ECAE process at 135°, finite element analysis was carried out. A physically-based viscohyperelastic-viscoplastic constitutive model was successfully implemented into a finite element code using (Marc-MSC). The study revealed the following:

- This model provides a good agreement with our measurements and reproduces properly the response of PC.
- The effect of speed and homogeneity of plastic deformation was observed. The faster the ram speed is, the lower the homogeneity of the equivalent plastic strain distribution is and the influence is slight.
- Analysis of stress fields of intermoleculire network moléculaie showed a state of multiaxial stress and inhomogeneous at the end of the extrusion at **10^{-2} (s^{-1})**
- The results of the distribution of plastic deformation have been estimated and their evolution was found in correlation with the results from literature.

References

[1] Segal VM, Reznikov VI, Drobyshevskiy AE, Kopylov VI. Russ Metall 1, 99-105, (1981).

[2] Campbell B, Edward G. Plastics Rubb Compos 28, 467–475, (1999).

[3] Zairi F, Aour B, Gloaguen JM, Nait-Abdelaziz M, Lefebvre JM. Comp Mater Sci 38, 202–216, (2006).

[4] Aour B, Zairi F, Nait-Abdelaziz M, Gloaguen JM, Rahmani O, Lefebvre JM. Int JComp Mater.sci 37, 491-506, (2006).

[5] Aour B, Zairi F, Nait-Abdelaziz M, Gloaguen JM, Rahmani O, Lefebvre JM. Mech.sci 50, 589-602, (2008).

[5] Aour B, Zairi F, Nait-Abdelaziz M, Gloaguen JM, Rahmani O, Lefebvre JM. Int JComp Mater.sci 45, 646-652, (2009).

[6] Li CKY, Xia ZY, Sue HJ. Polymer 41, 6285–93, (2000).

[7] Sue HJ, Dilan H, Li CKY. Polym Eng Sci 39, 2505–15, (1999).

[8] Sue HJ, Li CKY. J Mater Sci Lett 17, 853–6, (1998).

[9] Xia Z, Sue HJ, Hsieh AJ. J Appl Polym Sci 79, 2060–6, (2001).

[10] Ma J, Simon GP, Edward GH. Macromolecules 41, 409–20, (2008).

[11] R. Boulahia, J.M. Gloaguen, F. Zaïri, M. Naït-Abdelaziz, R. Seguela, T. Boukharouba, J.M. Lefebvre, Polym. 50, 5508-5517, (2009).

[12] Zairi F, Aour B, Gloaguen JM, Nait-Abdelaziz M, Lefebvre JM. Scripta Mater 56, 105–108, (2007).

[13] Xia Z, Sue HJ, Hsieh AJ, Huang JWL. J Polym Sci Part B: Polym Phys 39, 1394–403, (2001)..

[14] Terry S, creasy, Yoosin S, Kang ; Mater.Process.Technology 160, 90-98, (2005).

[15] Xia Z, Hartwig T, Sue HJ. J Macromol Sci Part B 43, 385–403, (2005).

[16] Weon JI, Creasy TS, Sue HJ, Hsieh AJ. Polym Eng Sci 45, 314–24, (2005).

[17] E.H. Lee, J. Appl. Mech. 36, 1-6, (1969).

[18] F. Sidoroff, J. Mécanique 13, 679-713, (1974).

[19] M.C. Boyce, S. Socrate, P.G. Llana, Polym. 41, 2183-2201, (2000).